IEEJ Transactions on xx
Vol.131 No.1 pp.1–11 DOI: 10.1541/ieejxxs.131.1

Paper

System Integration and Control for 3D Scanning Laser Metrology

Ernst Csencsics*a) Non-member, Shingo Ito* Non-member
Johannes Schlarp* Non-member, Georg Schitter* Non-member

Mechatronic imaging systems, ranging from nanoscale metrology to telescope systems and adaptive optics for astronomy, are complex machines that demand continual improvement of system speed, range, and precision. This demand requires advanced designs of the mechatronic components and a motion control scheme that carefully considers the interplay of a physical plant and the target application. A proper data acquisition system is required to synchronously acquire and process measurement and position data, and a sophisticated system integration is needed to obtain the maximum performance of the resulting system. This paper discusses the interplay between process and control design, as well as the system integration with the example of a scanning laser triangulation system for high precision 3D metrology. The integration process can be tailored to individual applications, and is discussed for raster and Lissajous scan trajectories, considering their individual requirements for the system and control design. Further it is demonstrated how these individually tailored system components can improve the performance in terms of precision and efficiency by several orders of magnitude.

Keywords: Mechatronic imaging systems, system integration, scanning laser metrology, model based control, iterative learning control

1. Introduction

The high-tech industry requires in various applications mechatronic systems with extreme performance in terms of precision and speed. Precision engineering is an important field of research for the continuous development of mechatronic imaging systems, such as atomic force microscopes (AFM) [1], wafer scanners [2], adaptive optics [3], and scanning laser metrology and microscopy [4] [5], in order to further improve the performance of these systems and machines.

What is common to all of these applications is the combination of precision motion control, a high dynamic range of several orders of magnitude, and a well-timed and synchronized data acquisition and control system for recording the independent sensor information, in case of metrology applications [6] [7], or for the manipulation of light beams, e.g. in projection systems [8].

Mechatronic imaging systems for future applications require even higher performance in terms of positioning bandwidth, actuation range, imaging speed, and precision. This can be achieved by advanced mechatronic designs and highly sophisticated motion control. Already at the system design phase all system components involved in the specific application have to be considered, such that a well predictable behavior of each component is required [9]. Examples for these components are the mechanical structure of the positioning system, the power amplifiers, the actuators, the sensors, electronics, and the real-time control system. A proper system integration, utilizing the interplay between process design and control design, allows optimizing the performance of the mechatronic imaging system for the specific application.

For nano-metrology applications, AFMs are a very important tool for imaging on the atomic and molecular level. However, the scanning based measurement in AFM is a limiting factor for the imaging speed of those systems. By improved mechatronic design and system integration the imaging speed of AFMs has been improved by three orders of magnitude [1], which includes a novel design of the AFM scanning unit [10] as well as modern control methods [7] [11].

In confocal laser scanning microscopy adaptive optics and improved motion control of the scanning mirrors enabled a significant improvement in imaging resolution [12] as well as a 70-fold reduction of the tracking error [4] when scanning at high speeds.

For automation and manufacturing processes optical sensors play an increasingly important role, due to high acquisition speeds, non-contact principles and therefore non-destructiveness, and simultaneous measurements in more than one dimension [13]. Even though tactile and other non-optical metrology systems proved themselves successful over the last decades, they are progressively replaced for high precision applications by e.g. laser triangulation or chromatic confocal sensors [14]. In addition, sub-micrometer accurate 3D measurement sensors become more and more important in the application of consumer products [15]. This paper presents the system design and integration of a laser triangulation 3D metrology system by combining the optical sensor system with a highly tailored opto-mechatronic scanner unit. In Section 2 a short overview over the main tasks in scanning metrology systems is given, followed by an introduction of the principle of the scanning optical metrology system. Sec-

a) Correspondence to: csencsics@acin.tuwien.ac.at
* The authors are with the Christian Doppler Laboratory for Precision Engineering for Automated In-Line Metrology at the Automation and Control Institute, Technische Universitat Wien, A-1040 Vienna, Austria.

tion 3 and Section 4 deal with the integrated approach of application targeted design by designing and tailoring the optomechatronic scanner unit and the motion control scheme for raster and Lissajous trajectories, respectively, and demonstrating the performance improvements. Section 5 presents the prototype of a flexible 3D scanning laser metrology system and its performance. Section 6 concludes the paper.

2. Scanning Optical 3D Metrology

2.1 Main Tasks in Scanning Metrology Systems

Independent of the individual imaging device the function of a scanning metrology system can be split up into three main tasks. The first is providing the scanning motion in X- and Y-direction in order to enable the measurement of an area of interest instead of just a single point. The second is the actual metrology task for obtaining the spatially resolved sensor information. The third main task is the synchronized data acquisition for recording the metrology sensor information as a function of the position in the X-Y plane, encoding and processing the metrology sensor data and generating a false-color 3D image.

The task of scanning can be performed by moving the sample under test, which is common in some AFM designs [6], by moving the metrology sensor [16], or in case of optical metrology by scanning e.g. the laser [8]. The achievable resolution and imaging speed is, next to the fundamental limits of the actual metrology sensing principle, given by the achievable precision and bandwidth of the scanning unit. For the actuation typically piezoelectric [10] or electromagnetic actuators [8] [9] are used, determining the actuation force, scanning speed and range of the scanning unit. In most scanning systems, the position is monitored by position sensors, which determine the achievable resolution. The proper integration of the actuators and sensors in the mechanical structure of the scanning unit determines the performance that can be achieved by the motion control system [9]. To control the scanner motion, in order to precisely follow the desired scan trajectory, open-loop control schemes, for open-loop stable systems [6], closed-loop control [8], two-degree-of-freedom control [11], or repetitive [17] and learning-based approaches [4] [18] can be applied.

The actual metrology task is determined by the employed measurement tool, which can be based on tactile or non-contact optical sensing principles. In tactile systems, such as AFMs, a determining factor for the imaging quality is the interaction between tip and sample. The shape of the used tip e.g. may result in measurement artifacts that need to be identified and compensated [19]. In the case of optical sensor principles the interaction of the used laser/light beam with the sample surface is a performance determining factor. The intensity of the back-scattered light is particularly relevant for the signal to noise ratio of the sensor [20]. Further the spot diameter and the achievable sampling rate are critical factors for the achievable spatial resolution of the entire metrology system [13]. Lag times due to signal processing in the optical sensor need to be considered for the design of the data acquisition system to guarantee synchronized data vectors.

The task of a well synchronized data acquisition is critical, as the system acquires the data vectors of the scanner position and the actual measurement and relates them accordingly. If the positions and the actual measurements show e.g. a constant shift, then image artifacts such as blurred feature shapes may be obtained in the fast scanning direction [21]. To avoid such a mismatch the data acquisition system needs to systematically consider all delays in the system, such as lag times due to signal processing in the optical sensor. This also entails the desire for all delays in the system being predictable and constant. To compensate for systematic measurement errors that result from the system geometry or the used scanner design, correction algorithms to remove e.g. scanner bow or plane tilt need to be implemented.

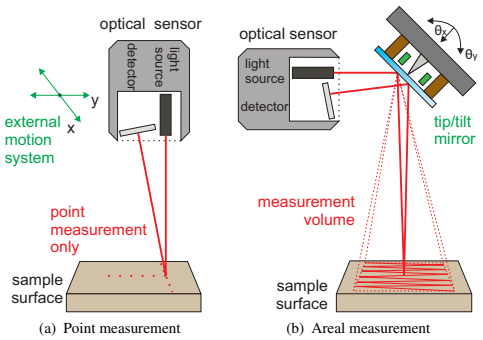

(a) Point measurement (b) Areal measurement

Fig. 1. Principle of integrating a triangulation sensor with a FSM system. Redirecting the optical path enables an advancement from (a) single point to (b) areal measurements.

2.2 Advancing Optical Point Sensors to 3D Metrology

In contrast to point-wise measuring scanning systems using a tactile probe, an optical metrology system does not have to be moved entirely to scan a sample. Instead the respective sensor system can remain stationary, while only the light path of the optical system is manipulated (Fig. 1(b)), which can be an enabler for improving measurement speeds, precision and versatility of optical metrology systems.

By integrating optical metrology sensors with optomechatronic components, e.g. fast steering mirrors (FSMs), as shown in Fig. 1(b), motion control and measurement algorithms for real-time data processing, an optical point sensor, as shown in Fig. 1(a), could be advanced to a flexible 3D metrology tool [22]. Various imaging and manufacturing systems already incorporate a scanning laser or light beam. They are ranging from laser confocal sensor systems [23], confocal microscopy [5] and laser triangulation with fixed patterns [24] to selective laser melting or selective laser sintering in additive manufacturing processes [25] and laser welding processes [26].

FSM systems, as shown in Fig. 2 (Type: OIM101, Optics In Motion LLC, Long Beach, USA), are optomechatronic devices that enable tip and tilt motion (typically single degrees) of an attached mirror by a set of voice coil actuators and include internal sensors for position measurement and control. When using such a FSM to deflect a laser or light beam for the 2-dimensional scanning of an area of interest within a 3D optical scanning metrology system, motion control by means of feedback is used to ensure a precise scanning motion and a high tracking performance in lateral direction [27]. In the sense of an integrated system design, such feedback controllers and

Post-print version of the article: E. Csencsics, S. Ito, J. Schlarp and G. Schitter, "System Integration and Control for 3D Scanning Laser Metrology," *IEEJ Transactions on Industrial Applications*, vol. 8, no. 2, p. 207-217, 2019. DOI: 10.1541/ieejjia.8.207

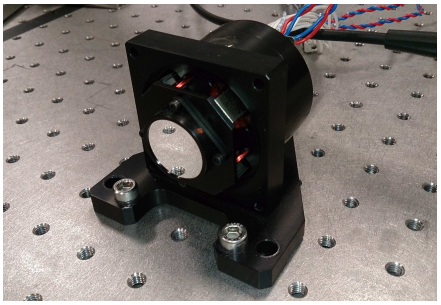

Fig. 2. State of the art fast steering mirror system from Optics in Motion. The 1 inch diameter mirror is actuated by two voice coils per axis and has a range of ± 26.2 mrad. The internal sensor system measures the mirror position in tip and tilt.

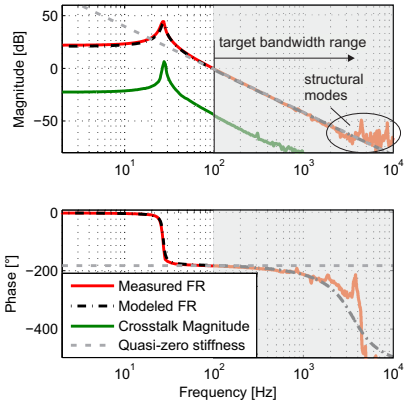

Fig. 3. Frequency response of a low stiffness FSM and a generic quasi-zero stiffness mechatronic system (dashed gray). The response of one FSM axis (solid red) is shown together with the fitted system model (dashed black) and the measured crosstalk (solid green) [27].

also the structure of the scanner should be tailored to the desired application task in order to maximize the entire system performance. This can be done by e.g. determining the scan trajectory that is best suited for the targeted application up front and tailoring the system and control structure accordingly.

3. System and Control Design for Raster Trajectories

The most commonly used type for scanning a 2-dimensional area is the raster trajectory [28] [29], which is also applied in numerous scientific instruments, e.g. scanning probe microscopy [6], and manufacturing processes. They result from driving the two system axes with one fast and one slow triangular signal, respectively. The raster trajectory provides a uniform spatial resolution over the entire scan area, resulting in a constant pixel clock when it comes to mapping the measured data to a reference grid. Although raster-based scanning is the principle mode for many scientific applications it often becomes a limiting factor of the overall throughput [30]. For a triangular reference signal at least the first 7-11 harmonics of the fundamental frequency should be covered by the system bandwidth [31]. For this reason typically controllers enabling a high closed-loop bandwidth are required, which can impose stringent requirements on the mechanical design of the FSM [32].

The frequency response of one axis of the low stiffness FSM in Fig. 2 is depicted in Fig. 3, together with its fitted model [27] and the crosstalk response. The FSM system is well designed, as first structural modes appear above 4 kHz and the phase lag due to sampling delay and low pass characteristic of the sensor is moderate, such that high control bandwidths up to 1 kHz appear feasible. The tip and tilt axes are also well decoupled with crosstalk being 40 dB lower than the axis TFs, justifying the use of single-input-single-output (SISO) controllers.

3.1 Alpha Tuning for PID Feedback Control

A frequently used controller type, which is due to the wide control bandwidth perfectly suited for raster trajectories, is the PID controller [33]. In order to intuitively tune the gains in the face of the tradeoff between robustness (stability margins, parameter variation) and performance (response time, tracking performance), which are typically the important properties of the closed-loop system in practical applications, the loop shaping based *Alpha tuning method* for the design of PID controllers has been proposed [34]. It is applicable to low stiffness and quasi-zero stiffness (Fig. 3) mechatronic systems that are showing a double integrator characteristic beyond the suspension mode and are typically controlled on their mass line (see gray area in Fig. 3). This system class includes many mechatronic positioning applications, ranging from wafer scanners [2] over CD player pickup heads to voice coil actuator based linear motion drives [35] and FSMs [27].

By using a suitable parametrization for the controller gains the *Alpha tuning method* reduces the number of design parameters to two: the open-loop cross-over frequency ω_c and a single tuning parameter α [34]. The cross-over frequency ω_c is usually either maximized for high performance, typically limited by structural modes of the positioned mass (beyond 3 kHz in Fig. 3), or fixed by the requirements of the respective application, e.g. the targeted trajectory in a scanning system. The tuning parameter α adjusts the spectral distance between the corner frequencies of the P-, I- and D-component that separate the control actions in the frequency domain and enables a direct tradeoff between performance and robustness of the closed-loop system [34]. An independent tuning of the controller gains is prevented, such that an overlapping and interference of control actions, mutually diminishing their desired action and the overall system performance, is avoided. Fig. 4 shows transfer functions (TFs) of controllers for the low stiffness FSM (see Fig. 3) for a target cross-over frequency f_c = 400 Hz and α-values of 2, 3, and 4.5. Higher α-values increase the phase margin and also the controller gain at high frequencies while decreasing the gain at low frequencies. This means that for large values of α the system becomes more robust, but the disturbance rejection and tracking performance at low frequencies is reduced due to

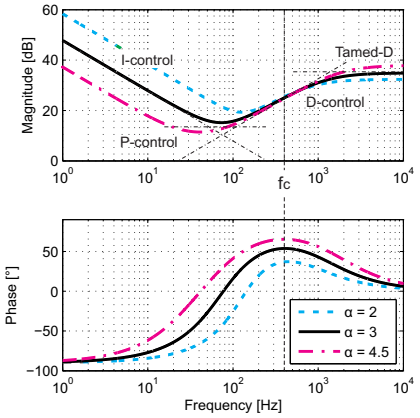

Fig. 4. Influence of the tuning parameter α on the TF of the resulting controller. The controllers for α-values of 2, 3 and 4.5 are shown [34].

the lower loop gain. The increased gain at higher frequencies additionally leads to an increased sensor noise feedback. Lower α-values have the inverse effects as they increase the performance at low frequencies and reduce the sensor noise feedback at the cost of a degraded robustness (lower phase margin). The value $\alpha = 3$ represents a good tradeoff between robustness (phase margin of 54°) and performance of the closed-loop controlled low stiffness FSM system [34].

Despite the PID controller being well suited for raster trajectories due to its wide control bandwidth, it does so far not particularly exploit the entire properties of the target trajectory. Extending the integrated design approach to also considering frequency-selective learning-based control schemes already at the integrated system design stage, can enable a significant improvement of the tracking performance.

3.2 Modeling-free Learning for Periodic Motion

High-precision periodic scanning motion can be realized by feedforward control but it typically requires a highly precise plant model [36]. When it is challenging to accurately identify the target system [37], modeling-free learning control can be used to simplify algorithms by learning at selected frequencies. The motion reference $r(t)$ of a scanning system, such as a raster trajectory, is typically periodic, such that it can be described by a Fourier series. This implies that the scanner tracking $r(t)$ needs good tracking performance only at the fundamental frequency f_r and its harmonics. To efficiently use this characteristic, inversion-based iterative control (IIC) [38] can update the control input $u(t)$ in the discrete frequency domain, learning from previous trials [39]. This is advantageous to decrease the required computation power to implement the algorithms [39] and to filter the measurement noise between the harmonic frequencies [37]. Modeling-free IIC has so far been successfully applied to piezoelectric actuated [40], hybrid reluctance actuated [41], and voice coil actuated scanner systems [37]. Fig. 5 shows the block diagram of the learning control structure. For learning in the discrete frequency domain, $r(t)$, $u(t)$ and the measured output $y(t)$ are

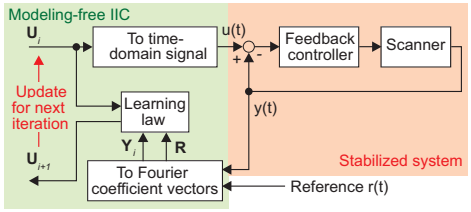

Fig. 5. Block diagram of the scanner regulated by feedback control and modeling-free IIC.

described by Fourier coefficient vectors

$$\mathbf{U} = [u_1 \dots u_k \dots u_q]^T, \quad \mathbf{Y} = [y_1 \dots y_k \dots y_q]^T, \cdots (1)$$

$$\mathbf{R} = [r_1 \dots r_k \dots r_q]^T, \quad \text{where } r_k = 0 \text{ for } k > q_r. \cdots (2)$$

The elements r_k, u_k and y_k are the corresponding complex Fourier coefficients [42] at the frequency of kf_r. To prevent the input saturation, $r(t)$ is band-limited by $q_r f_r$, and the IIC bandwidth is determined by using q as qf_r.

The learning law can be given in the form of Newton's method [37]:

$$\mathbf{U}_{i+1} = \mathbf{U}_i + \mathbf{J_a}^{-1}(\mathbf{R} - \mathbf{Y}_i), \cdots (3)$$

where the subscript i denotes the trial number, and $\mathbf{J_a}$ is a Jacobian matrix modeling the plant. While $\mathbf{J_a}$ may be found by system identification including model uncertainties for model-based IIC, it can be estimated during learning for modeling-free IIC. For this purpose, different types of algorithms have been proposed, such as the linear method [43], the secant method [40] and Broyden's method [37][44]. The selection of the algorithm requires a tradeoff between accuracy and speed of the learning process, which is always dependent on the target systems [37]. After the update of the control input, the frequency-domain input is converted into the time-domain signal $u(t)$ for the next trial, as shown in Fig. 5.

For the given scanner case the modeling-free IIC with the secant method is designed to track a triangular motion reference, commonly used in raster scanning [37]. To enable a large scan range, a raster trajectory with a fundamental frequency of $f_r = 40$ Hz and harmonics up to $q_r = 11$ is used. The scanner is stabilized by a PID feedback controller [4] with a closed-loop bandwidth of about 300 Hz, resulting in a positioning resolution of 0.54 mdeg_{rms}. To track a triangular reference q is set to 15 to compensate for higher harmonics generated by small but present non-linearities of the scanner. At each trial, 15 periods of the triangular motion are recorded to calculate the Fourier confident vector Y for a sufficient frequency resolution without spectral leakage. In Fig. 6 the measured results are shown. When the scanner is regulated by the PID controller only, the tracking error $e(t) = r(t) - y(t)$ is periodic and larger than ±1°, as shown in Fig. 6(b). With the modeling-free IIC active the error can, however, be successfully decreased by more than 99.8% to below ±2 mdeg. The resulting RMS value of $e(t)$ is 0.6 mdeg_{rms}, which is close to the positioning resolution of the system. The spectrum of the tracking error in Fig. 6(c) clearly demonstrates that the modeling-free IIC is effective at the selected frequencies and thus can be tailored to a desired trajectory in the course of an integrated design approach.

Post-print version of the article: E. Csencsics, S. Ito, J. Schlarp and G. Schitter, "System Integration and Control for 3D Scanning Laser Metrology," *IEEJ Transactions on Industrial Applications*, vol. 8, no. 2, p. 207-217, 2019. DOI: 10.1541/ieejjia.8.207

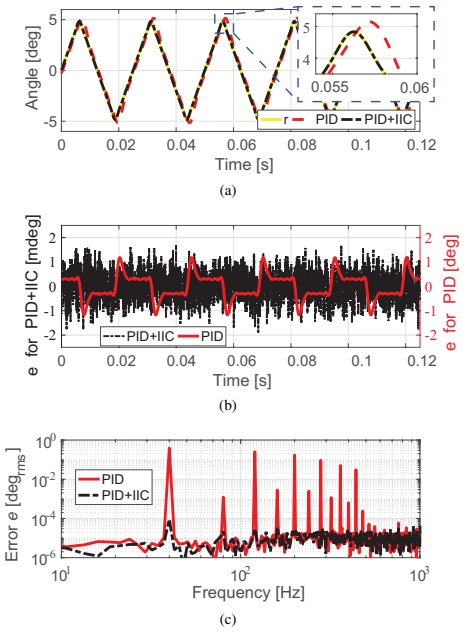

Fig. 6. 40 Hz scanning motion enhanced by IIC. (a) shows the measured angle y and the motion reference r. (b) depicts the tracking error ($e = r - y$) in the time domain. Note that the scaling differs by one order of magnitude. In (c) the error is shown in the frequency domain [37].

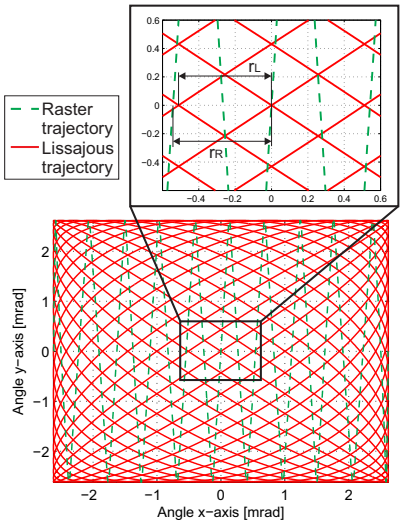

Fig. 7. Comparison of a raster (solid red) and a Lissajous trajectory (dashed green) for performing a 2-dimensional scan of an area. The fast axis of the raster scan is set to 10 Hz and the Lissajous frequencies are set to f_x =19 Hz and f_y =14 Hz, resulting in an equal frame rate and an almost equal spatial resolution r_R for the raster and r_L for the Lissajous scan (zoomed image) [27].

4. System and Control Design for Lissajous Trajectories

Lissajous trajectories represent an alternative to raster trajectories and have recently been proposed for precision scanning systems such as AFMs [30]. They result from driving each system axis with a sinusoidal signal of a fixed frequency, with the drive frequencies determining the spatial resolution and the frame rate [45]. The spatial resolution of a Lissajous scan is non-uniform, being higher in the outer areas of the scan area and lowest in the center. The maximum distance between two intersections of the scan trajectory and the principle axes (see Fig. 7) can serve as simple and efficient metric for this nonuniform resolution. The spatial resolution is building up gradually with evolving scan time, being termed multi-resolution and providing an overview of the entire scan are after a fraction of the scan time. This may be a particularly valuable property for high speed metrology systems in industrial applications.

Fig. 7 shows a comparison of an exemplary raster and a Lissajous scan trajectory. With the chosen raster (10/0.5 Hz) and Lissajous frequencies (19/14 Hz), trajectories with almost equal spatial resolution at a rate of 1 frame/s are obtained.

4.1 Dual Tone Feedback Control

The required large control bandwidth for raster trajectories imposes strict requirements on the mechanical design of the FSM system [32], and the tracking errors even with the best performing PID controller are still significant, especially at the turning points of the triangle [46]. Lissajous trajectories can relax these design challenges and improve the tracking performance. Under the assumption that the control task is the precise tracking of a defined Lissajous trajectory and no disturbance rejection capability at low frequencies is required, it is possible to shape the SISO feedback controller of each system axis to a single tone, with a high control gain localized at the sinusoidal drive frequency of the individual axis, which essentially corresponds to the internal model principle [30]. To also reject the small but present amount of inter-axis crosstalk in the system (see Fig. 3), dual tone (DT) controllers with a high controller gain localized around both driving frequencies have been proposed [27]. The controllers are obtained by H_∞ control synthesis [47], allowing the specification of requirements on the controller in a parametric way by using suitable weighting functions.

In Fig. 8(a) the TFs of the DT and a PID controller (designed for ω_c = 500 Hz and α = 3) are compared, showing with more than 45 dB significantly higher control gains of the DT controller at the Lissajous drive frequencies and lower gains at all other frequencies as compared to the PID controller. The complementary sensitivity functions for reference tracking of the resulting closed-loop systems are depicted in Fig. 8(b). The system with the PID controller has a control bandwidth of 730 Hz and is thus suitable for tracking a triangular reference signal of up to 100 Hz, with the first 7 harmonics covered. The PID controller can also be used for Lissajous trajectories with drive frequencies up to the control bandwidth. The system with the DT controller reaches the 0 dB line exactly at the two drive frequencies, while remaining below -40 dB at lower and higher frequency ranges.

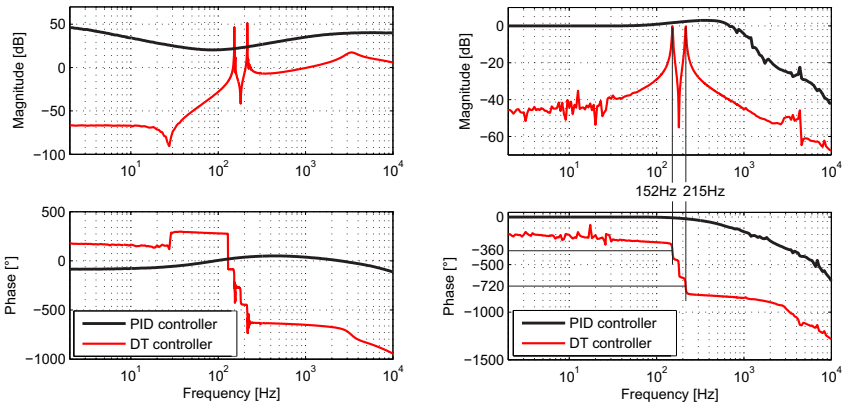

(a) Controller transfer functions (b) Complimentary sensitivity functions

Fig. 8. Comparison of the DT and PID controller. (a) shows the measured transfer functions of the implemented controllers. The DT controller shows high control efforts localized at both drive frequencies (152/215 Hz). (b) depicts the measured complimentary sensitivity function of the FSM for both controllers [27].

Employing a right half plane zero results in a perfect phase match of 360° and 720° at the drive frequencies.

Experiments show that the Lissajous scan (152/215 Hz) with the tailored DT controller results in a factor 40 smaller rms tracking error when compared to tracking the same Lissajous trajectory with the PID controller [27], which is explained by the mismatches in the phase and gain (peaking before the roll-off) at higher frequencies, as consequence of the PID design (see Fig. 8(b)). Comparing the conventional raster scan with the PID controller to the Lissajous scan with the DT controller, both trajectories having the same temporal and spatial resolution, shows a reduction of the tracking error by one order of magnitude. The rms current for actuation in the Lissajous/DT case is, however, significantly increased and more than 2.3 times higher than for the raster/PID case, which limits the range of high-resolution Lissajous scans with higher drive frequencies. This is due to the higher fundamental frequencies of the Lissajous scan, which are required to obtain the same spatial resolution as the raster trajectory.

Extending the level of system integration from the trajectory and control design further to the mechatronic system design of the FSM allows to mitigate limitations, such as the reduced scan range due to the higher current consumption.

4.2 Resonant FSM Design for Lissajous trajectories

The performance in terms of speed and range of a voice coil actuated FSM system (see Fig. 2), enabling a large angular range [48], is limited by the maximum actuator force, determined by the maximum permissible coil current. The first approach to relax this limitation can be to maximize the actuator's motor constant, but there will be a physical limit this actuation technology cannot exceed. Looking at the feedback control loop and its loop gain, as indicator for frequency ranges with good tracking performance, it can be seen that, if a certain loop gain is required at a defined frequency in order to result in a desired tracking performance, there is no difference how the loop gain is distributed over the plant and the controller. This means that the high controller gains of the DT controllers at the desired drive frequency, leading to high actuator currents, could also be redistributed to the plant gain of the FSM dynamics. Considering a system tailored for the continuous dynamic scan case, this can be achieved by retuning the resonance frequencies of the suspension mode for each axis to the desired drive frequency [8]. At the resonance the torque and angular velocity are in phase, such that the torque acts in the direction of the movement and thus maximizes the work [9]. By this approach the scanning motion of the FSM tracking the desired Lissajous trajectory can be performed with maximum efficiency.

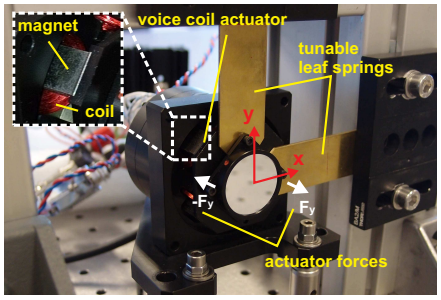

Fig. 9. Tuned FSM system. The spring constants of x- and y-axis are increased using tunable leaf springs. The resonance frequencies can be tuned by adjusting the length of each leaf spring [8].

The resonance frequency $\omega_0 = \sqrt{k_r/J}$ of a low stiffness FSM can be increased by either (i) reducing the system's inertia J, which lifts the mass line, or (ii) by increasing the rotational spring constant k_r of the guiding flexures, which lowers the spring line (see Fig. 10). An increase of the spring constant is easily feasible and a tunable mechanism that enables the adjustment of the exact resonance frequency can be attached to the existing system. Fig. 9 shows the setup of

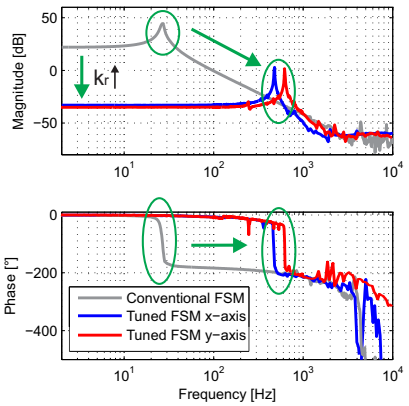

Fig. 10. Frequency responses of FSM systems. The frequency response of the tuned x- (blue) and y-axis (red) and the response of the conventional FSM system (gray) are shown. The resonance frequencies are shifted to f_{0x} = 473 Hz and f_{0y} = 632 Hz, respectively, and increase the plant gain by more than 30 dB [8].

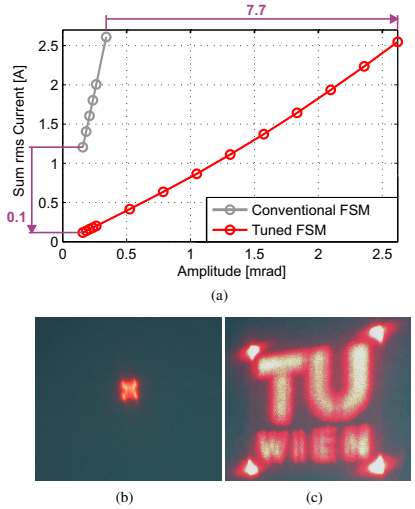

Fig. 11. Reduced current consumption and enlarged scan area. (a) compares the rms current for the conventional (black) and the tuned FSM system (red). (b) and (c) compare the images of a projection system using the conventional and the tuned FSM, respectively, to track the Lissajous reference at the respective maximum scan amplitude (0.34 mrad and 2.62 mrad) [8].

the tuned FSM with leaf springs of adjustable length to tune the resulting stiffness. The frequency response of the conventional FSM and the tuned FSM are depicted in Fig. 10. The resonance frequency of the x- and y-axis are tuned to f_{0x} = 473 Hz and f_{0y} = 632 Hz, respectively, by increasing the system stiffness by a factor of 512 and 630 as compared to the conventional FSM, resulting in a significantly higher plant gain at this frequency due to the low damping.

For comparison of the tuned and the conventional FSM, both systems are tracking the desired reference Lissajous trajectory with the related DT controllers, while increasing the scan amplitudes until the current limit of the actuator coils is reached. Fig. 11(a) depicts the current consumption of both FSM configurations and shows that the current consumption of the tuned FSM is 10 times smaller, denoting a reduction of dissipated energy in the coils by a factor of 100. Due to the reduced current consumption the tuned FSM also has a 7.7 times larger scan range, entailing an about 60 times larger scan area. In Fig. 11(b) and Fig. 11(c) the projected patterns of a laser projection system employing the conventional and the tuned FSM are shown, respectively, clearly illustrating the 60-fold increase in scan area when using the tuned FSM.

When tracking such a high resolution Lissajous trajectory, a precise phase matching between the reference and actual position is required in order to maintain the desired shape of the trajectory and particularly its spatial resolution [46]. The model-based DT feedback controllers developed previously, rely on highly accurate system models, especially of the phase (incl. delays, etc.) around the sharp resonances of the system. The measurement and modeling uncertainties of the system identification represent a potential limitation on the precision of the models and on the tracking performance of controllers tuned distinctly to the resonances. This limitation can be avoided by employing a phase-locked-loop (PLL) which does not require these precise models of the system phase.

4.3 PLL Control Scheme for Sinusoidal References

When it comes to tracking of sinusoidal signals, PLLs are a well established and frequently used control scheme [50], as they keep an output signal synchronized with a reference input in frequency and phase [51]. Originating from the fields of communication systems [52], radio and television [50], PLL have also been applied to several mechatronic systems [53] [54].

The PLL, as shown in Fig. 12, consists of a phase detector (PHD) a low pass filter (LP) and a voltage controlled oscillator (VCO). The PHD multiplies the reference and the output and generates a signal proportional to the phase error, as well a high frequency component which is eliminated by the LP. The VCO is a frequency modulated oscillator with its output frequency being a linear function of the LP output. With its central frequency set to the desired oscillation frequency it adjusts the output frequency to minimize the phase error. For establishing a precise phase relation between the reference and output position of a FSM, the mechatronic system is inserted into the PLL after the VCO (one PLL per axis), as depicted in Fig. 12, which makes the position of the mechatronic system the new output signal [49].

The mechatronic system comprises the FSM, with the axis TFs G_{xx} and G_{yy}, the crosstalk TFs G_{xy} and G_{yx}, and the optical position sensor PS, as well as the two current amplifiers. The measured mirror position is fed back to the PHD which modifies the VCO output, such that the phase error between the output signal $\Theta_{x/y}$ (mirror position) andthe reference signal $\Theta_{x/y,ref}$ is minimized.

As the PLL is only controlling the phase, the adaptive gains g_x and g_y are added after the VCO, which are automatically tuned to the inverse plant gain at the respective drive fre-

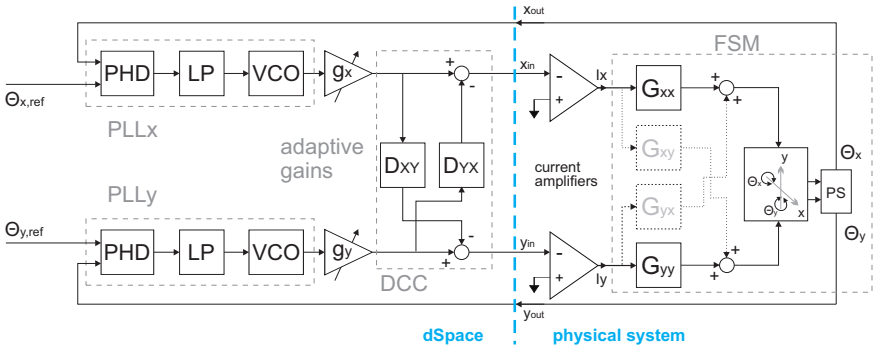

Fig. 12. Phase locked loop based control structure for the tracking of Lissajous trajectories. The phase of the output signal is synchronized with the input signal by one PLL per axis. The gains g_x and g_y are the tuned to the inverted plant gains to scale the amplitude of the output to the amplitude of the reference. The DCC blocks D_{xy} and D_{yx} are used to remove crosstalk at the drive frequencies [49].

quency. The PLLs are, however, not capable of rejecting disturbances that result from the crosstalk between the axes. As the crosstalk behavior is repeatable, it can be seen as a measurable external disturbance, such that decoupling control (DCC) can be used to compensate it [55]. Decouplers that compensate the crosstalk, are designed by

$$D_{xy}(s) = \left.\frac{G_{xy}(s)}{G_{yy}(s)}\right|_{s=j\omega_x}, D_{yx}(s) = \left.\frac{G_{yx}(s)}{G_{xx}(s)}\right|_{s=j\omega_y} \cdots\cdot (4)$$

with G_{xy} and G_{yx} being the models of the crosstalk frequency responses.

Experiments were run with the tuned FSM tracking a high resolution Lissajous trajectory with reference frequencies of 473 Hz and 632 Hz using the PLL control structure and comparing the tracking error to the error with tailored DT controllers. It is demonstrated that with PLL control the tracking error is reduced by additional 60% as compared to the case with DT control (data not shown), while both control structures achieve the same performance in terms of energy consumption and maximum scan range [49].

5. Application of 3D Optical Metrology

By integration of an optical metrology sensor with an optomechatronic scanner unit, such as a FSM, and a data acquisition system with appropriate measurement algorithms for real-time data processing, a flexible 3D scanning laser metrology system can be obtained. According to the concept shown in Fig. 1(b) a prototype of a scanning laser-triangulation sensor is developed. The scanning sensor prototype, shown in Fig. 13, consists of a laser triangulation sensor (Type: ILD 2300-100, Micro-Epsilon GmbH, Germany), with a measurement range of 100 mm and a FSM (Type: OIM102, Optics In Motion LLC, Long Beach, USA), for scanning the measurement point over the sample surface. To record a three dimensional image of the sample, the transmission and the reflection path of the triangulation sensor are manipulated by the FSM [16]. Therefore, this setup satisfies the Scheimpflug condition [20] which entails a sharp projection of the diffusely reflected laser point from the sample onto the detector. With the geometrical relations of the setup, the surface profile of a sample can be reconstructed

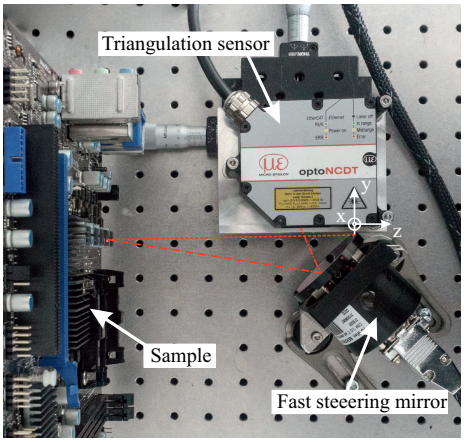

Fig. 13. Experimental setup of the scanning laser triangulation sensor. With a tip-tilt mirror the optical paths of the triangulation sensor are manipulated.

from the sensor measurement and the angular position of the FSM [16], which simultaneously also removes the scanner bow. To correct for a tilted sample plane a RANSAC algorithm, which detects and subtracts a flat surface, is used [56]. Lissajous-based scan trajectories with driving frequencies of $f_1 = 27$ Hz and $f_2 = 52$ Hz are applied to the metrology system to scan the sample, utilizing DT controllers for the scanning axes of the FSM [8]. The resulting measurement system has a scan area of 16 x 16 x 100 mm and provides resolutions of 900 x 900 x 30 μm for the respective x-, y- and z-axis.

In Fig. 14 the measured sample surface of a Nanoblock (Kawada Co. Ltd., Tokyo, Japan), scanned with the described Lissajous trajectory at a frame rate of 1 frame/s, are shown. The measurement result shows good agreement with reference measurements obtained by a linearly scanned line sensor (data not shown). The two features on the left are cut of due to the limited scan area.

Another demand for future metrology systems is high flexibility. One typical use case in such measurement applications is for example that certain areas on a sample need to be

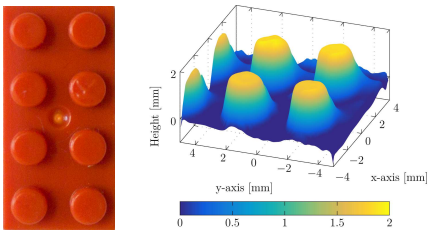

(a) Sample (b) Reconstructed surface profile

Fig. 14. Measurement result of the scanning triangulation sensor at a frame rate of 1 frame/s. (a) shows the nano block sample which has a dimension of 16 x 8 x 2 mm. (b) depicts the reconstructed surface profile, showing good agreement with the sample.

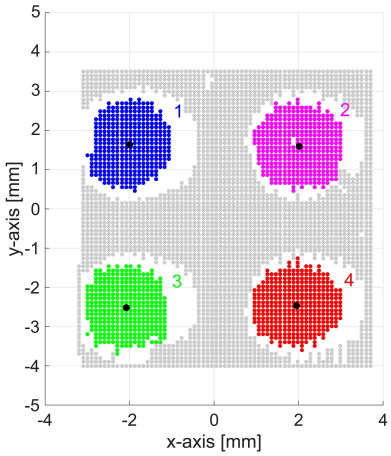

Fig. 15. Result of the clustering algorithm. All four features (cylinderical structures on the nano block) are individually detected. Also the center of gravity of each feature is depicted (black dot).

imaged with higher spatial resolution than the rest of the sample [20]. Instead of scanning the entire sample with the required higher spatial resolution, which would increase the measurement time, only the sub-area containing the feature of interest may be rescanned. This, however, requires the measurement system to adapt to the particular measurement task. This can be e.g. realized by using machine vision, instead of statically tailoring the trajectory to one defined sample or product by teaching procedures, enabling the recognition and adaptive rescan of relevant features on an arbitrary sample [57].

In particular an agglomerative clustering algorithm [58] is used to identify the centers of gravity and lateral dimensions of features obtained with a low resolution overview scan of the entire sample [57]. Fig. 15 shows the result of the clustering algorithm applied to the overview scan in Fig. 14b, which is obtained after 1.48 s. Each detected cluster, equalling an individual feature, is displayed in a different color and the calculated centers of gravity are marked by black dots. The cluster of the bottom plane is depicted in grey. White areas, without data points, indicate non-valid measurement data around the edges of the features e.g. due to shadowing effects. Compared to the image in Fig. 14b the clustering results in objects of similar shape, position and orientation. With the centers of gravity and the lateral dimensions the offset and scan amplitudes of the trajectories tailored for each feature can be determined [57]. In Fig. 16 the result of the rescan of feature No. 3 (green) is shown. As the same trajectory is used for the rescan, the spatial resolution is increased by a factor of 2 and 3 for the x- and y-axis, respectively, showing the feature of interest in higher detail.

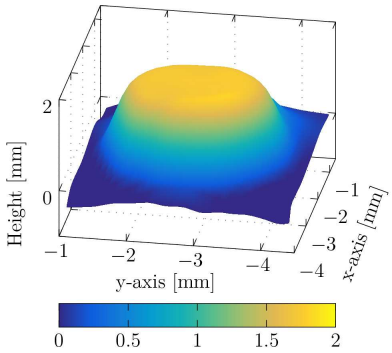

Fig. 16. Re-measured high resolution surface profile of the detected feature number 3 (green). The resolutions in x- and y-direction is increased by a factor 2 and 3, respectively. The frame rate is 1 frame/s.

In summary it is shown that the integrated mechatronic design of the FSM in combination with a laser triangulation sensor, an appropriate data acquisition system, and machine vision techniques forms a high performance optical 3D metrology system with high flexibility to the respective measurement task.

6. Conclusions

This paper demonstrates that considerable performance improvements of mechatronic imaging systems can be achieved by an integrated mechatronic design in combination with sophisticated motion control. A proper system integration with focus on the target application, utilizing the interplay between process design and control design, allows optimizing the performance of the mechatronic imaging system for the specific application. The performance improvement is demonstrated for the example of a FSM in a scanning optical 3D metrology system. Extending PID feedback control for tracking raster trajectories by a modeling-free iterative learning-based control scheme, being frequency-selective to the harmonics of the target trajectory, the tracking error is reduced by more than 99.8%. By tailoring feedback controllers to the properties of a pre-defined Lissajous trajectory, the tracking error can be reduced by one order of magnitude as compared to the conventional combination of a raster trajectory and a PID controller. Considering also the FSM dynamics and tuning the axis resonances to the reference frequencies, the current consumption can be reduced by a factor of 10 compared to a conventional FSM. Vice-versa the scan area of the tuned FSM is increased by a factor of 60. The final integration of the FSM, the laser triangulation sensor, and the real-time control and data acquisition system demonstrates

Post-print version of the article: E. Csencsics, S. Ito, J. Schlarp and G. Schitter, "System Integration and Control for 3D Scanning Laser Metrology," *IEEJ Transactions on Industrial Applications*, vol. 8, no. 2, p. 207-217, 2019. DOI: 10.1541/ieejjia.8.207

that a high precision 3D metrology system can be obtained. The required flexibility of the metrology system to adapt to individual measurement tasks is enabled by machine vision techniques that enable a recognition and adaptive rescan of individual features. Future work includes an integration and combination of the developed methods and systems also with other optical sensing principles, like confocal sensors, in order to obtain compact and versatile high performance metrology tools for future production systems. This also includes particularly the development of intelligent measurement algorithms that can be used to generate additional information about the sample from the measured areal data.

Acknowledgements

The financial support by the Austrian Federal Ministry for Digital, Business and Enterprise, and the National Foundation for Research, Technology and Development, as well as MICRO-EPSILON MESSTECHNIK GmbH & Co. KG and ATENSOR Engineering and Technology Systems is gratefully acknowledged.

References

(1) P. Hansma, G. Schitter, G. Fantner, and C. Prater, "High speed atomic force microscopy," *Science*, vol. 314, pp. 601–602, 2006.
(2) H. Butler, "Position control in lithographic equipment," *IEEE Control Systems Magazine*, vol. 31, no. 5, 2011.
(3) R. K. Tyson, *Principles of adaptive optics*. CRC press, 2015.
(4) H. W. Yoo, S. Ito, and G. Schitter, "High speed laser scanning mircoscopy by iterative learning control of a galvanometer scanner," *Control Engineering Practice*, vol. 50, pp. 12–21, 2016.
(5) S. Arunkarthick, M. M. Bijeesh, A. S. Vetcha, N. Rastogi, P. Nandakumar, and G. K. Varier, "Design and construction of a confocal laser scanning microscope for biomolecular imaging," *Current Science*, vol. 107, no. 12, pp. 1965–1969, 2014.
(6) G. Schitter, P. J. Thurner, and P. K. Hansma, "Design and input-shaping control of a novel scanner for high-speed atomic force microscopy," *Mechatronics*, vol. 18, no. 5, pp. 282–288, 2008.
(7) S. Kuiper and G. Schitter, "Model-based feedback controller design for dual actuated atomic force microscopy," *Mechatronics*, vol. 22, no. 3, pp. 327–337, 2012.
(8) E. Csencsics and G. Schitter, "System design and control of a resonant fast steering mirror for lissajous-based scanning," *IEEE Transactions on Mechatronics*, vol. 22, no. 5, pp. 1963–1972, 2017.
(9) R. Munnig Schmidt, G. Schitter, A. Rankers, and J. van Eijk, *The Design of High Performance Mechatronics*, 2nd ed. Delft University Press, 2014.
(10) G. Schitter, K. J. Astrom, B. E. DeMartini, P. J. Thurner, K. L. Turner, and P. K. Hansma, "Design and modeling of a high-speed afm-scanner," *IEEE Transactions on Control Systems Technology*, vol. 15, no. 5, pp. 906–915, 2007.
(11) G. Schitter, A. Stemmer, and F. Allgwer, "Robust two-degree-of-freedom control of an atomic force microscope," *Asian Journal of Control*, vol. 6, no. 2, pp. 156–163, 2004.
(12) H. Yoo, M. E. van Royen, W. A. van Cappellen, A. B. Houtsmuller, M. Verhaegen, and G. Schitter, "Automated spherical aberration correction in scanning confocal microscopy," *Review of Scientific Instruments*, vol. 85, p. 123706, 2014.
(13) K. Harding, *Handbook of Optical Dimensional Metrology*. Taylor & Francis, 2013.
(14) J. Salzberger, "Optisch, berührungslos, präzise - Optische Messtechnik für die Qualitätssicherung im Prozess," *Laser + Photonik*, vol. 4, pp. 50–53, 2013.
(15) F.-A. Vision, *Marktstudie 3-D-Messtechnik in der deutschen Automobil- und Zulieferindustrie*. Fraunhofer Verlag, Stuttgart, 2009.
(16) J. Schlarp, E. Csencsics, and G. Schitter, "Optical scanning of a laser sensor for 3d imaging," *IEEE Transactions on Instrumentation and Measurement, submitted*, 2018.
(17) M. Steinbuch, S. Weiland, and T. Singh, "Design of noise and period-time robust high-order repetitive control, with application to optical storage," *Automatica*, vol. 43, no. 12, pp. 2086–2095, 2007.
(18) K. K. Leang and S. Devasia, "Design of hysteresis-compensating iterative learning control for piezo-positioners: Application to atomic force microscopes," *Mechatronics*, vol. 16, no. 3-4, pp. 141–158, 2006.
(19) J. Shen, D. Zhang, F. Zhang, and Y. Gan, "Afm tip-sample convolution effects for cylinder protrusions," *Applied Surface Science*, vol. 422, pp. 482–491, 2017.
(20) A. Donges and R. Noll, *Laser measurement technology*. Atlanta: Springer, 2015.
(21) S. Ito, M. Poik, E. Csencsics, J. Schlarp, and G. Schitter, "Scanning chromatic confocal sensor for fast 3d surface characterization," *ASPE/euspen Summer Topical Meeting on Advancing Precision in Additive Manufacturing*, submitted, 2018.
(22) M. Rioux, "Laser range finder based on synchronized scanners," *Applied Optics*, vol. 23, no. 21, pp. 3837–3844, 1984.
(23) K. Noda, N. Binh-Khiem, Y. Takei, T. Takahata, K. Matsumoto, and I. Shimoyama, "Multi-axial confocal distance sensor using varifocal liquid lens," in *17th International Conference on Solid-State Sensors, Actuators and Microsystems*, Barcelona, 2013, pp. 1499–1502.
(24) P. GmbH. (2017, Mai) Perceptron Helix. [Online]. Available: https://perceptron.com/helix-sensor/
(25) A. J. Pinkerton, "Lasers in additive manufacturing," *Optics & Laser Technology*, vol. 78, pp. 25–32, 2016.
(26) W. Huang and R. Kovacevic, "A laser-based vision system for weld quality inspection," *Sensors*, vol. 11, no. 12, pp. 506–521, 2011.
(27) E. Csencsics, R. Saathof, and G. Schitter, "Design of a dual-tone controller for lissajous-based scanning of fast steering mirrors," *2016 American Control Conference, Boston, MA, USA*, 2016.
(28) L. R. Hedding and R. A. Lewis, "Fast steering mirror design and performance for stabilization and single axis scanning," *SPIE Vol. 1304 Acquisition, Tracking and Pointing IV*, pp. 14–24, 1990.
(29) S. Xiang, S. Chen, X. Wu, D. Xiao, and X. Zheng, "Study on fast linear scanning for a new laser scanner," *Optics & Laser Technology*, vol. 42, no. 1, pp. 42–46, Feb 2010.
(30) T. Tuma, J. Lygeros, V. Kartik, A. Sebastian, and A. Pantazi, "High-speed multiresolution scanning probe microscopy based on lissajous scan trajectories," *Nanotechnology*, vol. 23, no. 18, p. 185501, 2012.
(31) A. J. Fleming and A. G. Wills, "Optimal periodic trajectories for band-limited systems," *IEEE Transactions on Control Systems Technology*, vol. 17, no. 3, p. 552, 2009.
(32) M. Sweeney, G. Rynkowski, M. Ketabchi, and R. Crowley, "Design considerations for fast steering mirrors (fsms)," *Optical Scanning 2002, Proceedings of SPIE*, vol. 4773, 2002.
(33) D. J. Kluk, M. T. Boulet, and D. L. Trumper, "A high-bandwidth, high-precision, two-axis steering mirror with moving iron actuator," *Mechatronics*, vol. 22, no. 3, pp. 257–270, Apr 2012.
(34) E. Csencsics and G. Schitter, "Parametric pid controller tuning for a fast steering mirror," *1st IEEE Conference on Control Technology and Applications, Kohala Coast, Hawaii, USA*, 2017.
(35) S. Ito, J. Steininger, and G. Schitter, "Low-stiffness dual stage actuator for long rage positioning with nanometer resolution," *Mechatronics*, vol. 29, 2015.
(36) K. K. Leang, Q. Zou, and S. Devasia, "Feedforward control of piezoactuators in atomic force microscope systems," *IEEE Control Systems Magazine*, vol. 29, no. 1, pp. 70–82, Feb 2009.
(37) S. Ito, H. W. Yoo, and G. Schitter, "Comparison of modeling-free learning control algorithms for galvanometer scanner's periodic motion," in *IEEE International Conference on Advanced Intelligent Mechatronics*, July 2017, pp. 1357–1362.
(38) S. Tien, Q. Zou, and S. Devasia, "Iterative control of dynamics-coupling-caused errors in piezoscanners during high-speed AFM operation," *IEEE Transactions on Control Systems Technology*, vol. 13, no. 6, pp. 921–931, Nov 2005.
(39) M. Hehn and R. D'Andrea, "A frequency domain iterative learning algorithm for high-performance, periodic quadrocopter maneuvers," *Mechatronics*, vol. 24, no. 8, pp. 954 – 965, 2014.
(40) Y. Li and J. Bechhoefer, "Model-free iterative control of repetitive dynamics for high-speed scanning in atomic force microscopy," *Review of Scientific Instruments*, vol. 80, no. 1, p. 013702, 2009.
(41) S. Ito, S. Troppmair, B. Lindner, F. Cigarini, and G. Schitter, "Long-range fast nanopositioner using nonlinearities of hybrid reluctance actuator for energy efficiency," *IEEE Transactions on Industrial Electronics*, in press, 2018.
(42) H. P. Hsu, *Schaum's Outline of Signals and Systems*, 3rd ed. McGraw-Hill Education, 2014.
(43) K. S. Kim and Q. Zou, "A modeling-free inversion-based iterative feedfor-

Post-print version of the article: E. Csencsics, S. Ito, J. Schlarp and G. Schitter, "System Integration and Control for 3D Scanning Laser Metrology," *IEEJ Transactions on Industrial Applications*, vol. 8, no. 2, p. 207-217, 2019. DOI: 10.1541/ieejjia.8.207

ward control for precision output tracking of linear time-invariant systems," *IEEE/ASME Transactions on Mechatronics*, vol. 18, no. 6, pp. 1767–1777, Dec 2013.
(44) T. Sauer, *Numerical Analysis*, 2nd ed. Pearson, 2011.
(45) T. Tuma, J. Lygeros, A. Sebastian, and A. Pantazi, "Optimal scan trajectories for high-speed scanning probe microscopy," *2012 American Control Conference*, 2012.
(46) E. Csencsics, "Integrated design of high performance mechatronics for optical inline metrology systems," Ph.D. dissertation, Technische Universität Wien, Vienna, Austria, 2017.
(47) S. Skogestad and I. Postlethwaite, *Multivariable Feedback Control*. John Wiley, New York, 2005.
(48) M. Hafez and T. C. Sidler, "Fast steering two-axis tilt mirror for laser pointing and scanning," *SPIE Vol. 3834*, September 1999.
(49) E. Csencsics and G. Schitter, "Design of a phase-locked-loop-based control scheme for lissajous-trajectory scanning of fast steering mirrors," *2017 American Control Conference, Seattle, WA, USA*, 2017.
(50) D. Abramovitch, "Phase-locked loops: A control centric tutorial," *Proceedings of the 2002 American Control Conference IEEE*, 2002.
(51) G.-C. Hsieh and J. C. Hung, "Phase-locked loop techniques. A survey," *IEEE Transactions on Industrial Electronics*, vol. 43, no. 6, p. 609, 1996.
(52) D. R. Stephens, *Phase-locked loops for wireless communications: digital, analog and optical implementations*. Springer Science & Business Media, 2007.
(53) A. Hung, H. Lai, T. Lin, S. Fu, and M. Lu, "An electrostatically driven 2d micro-scanning mirror with capacitive sensing for projection display," *Sensors and Actuators A: Physical*, vol. 222, p. 122, 2015.
(54) M. H. H. Mokhtar and R. R. A. Syms, "Resonant fiber scanner with optical feedback," *Optics Express,*, vol. 22, no. 21, p. 25629, 2014.
(55) X. Zhou, D. Wang, J. Wang, and S.-C. Chen, "Precision design and control of a flexure-based roll-to-roll printing system," *Precision Engineering*, vol. 45, p. 332, 2016.
(56) F. Tarsha-Kurdi, T. Landes, and P. Grussenmeyer, "Hough-transform and extended ransac algorithms for automatic detection of 3d building roof planes from lidar data," *ISPRS Workshop on Laser Scanning 2007 and SilviLaser 2007*, 2007.
(57) J. Schlarp, E. Csencsics, and G. Schitter, "Feature detection and scan area selection for 3d laser scanning sensors," *IEEE/ASME International Conference on Advanced Intelligent Mechatronic, submitted*, 2018.
(58) C. Steger, M. Ulrich, and C. Wiedemann, *Machine vision algorithms and applications*. John Wiley and Sons, 2018.

E. Csencsics (Non-member) Ernst Csencsics is postdoctoral researcher at the Automation and Control Institute (ACIN) at Vienna University of Technology. He received a MSc. and PhD degree in Electrical Engineering from TU Wien, Austria in 2014 and 2017, respectively. His primary research interests are on high performance mechatronic systems design, control of opto-mechatronic systems, precision engineering, and in-line metrology systems.

S. Ito (Non-member) Shingo Ito received the MASc in Mechanical and Industrial Engineering from the University of Toronto, Canada, in 2007 and the PhD in Electrical Engineering from TU Wien, Vienna, Austria in 2015. From 2007 to 2010, he served as an engineer in the field of motion control at Yaskawa Electric Corporation, Iruma, Japan. He is currently a postdoctoral researcher at the Automation and Control Institute (ACIN), TU Wien. His research interest includes design and control of high-precision mechatronic systems for production, inspection and automation.

J. Schlarp (Non-member) Johannes Schlarp received an MSc. in Electrical Engineering from the Vienna University of Technology, Vienna, Austria in 2017 and is currently pursing a PhD degree with the Automation and Control Institute of the Vienna University of Technology, Vienna, Austria. His primary research interests are on high performance mechatronic systems and precision engineering for automated in-line metrology.

G. Schitter (Non-member) Georg Schitter is Professor for Advanced Mechatronic Systems at the Automation and Control Institute (ACIN) of TU Wien. He received an MSc in Electrical Engineering from TU Graz, Austria (2000) and an MSc and PhD degree from ETH Zurich, Switzerland (2004). His primary research interests are on high-performance mechatronic systems, particularly for applications in the high-tech industry, scientific instrumentation, and mechatronic imaging systems, such as AFM, scanning laser and LIDAR systems, telescope systems, adaptive optics, and lithography systems for semiconductor industry. He received the IFAC Mechatronics best paper award (2008 to 2011) and 2013 IFAC Mechatronics Young Researcher Award, and served as an Associate Editor for IFAC Mechatronics, Control Engineering Practice, and for the IEEE-Transactions on Mechatronics.

Post-print version of the article: E. Csencsics, S. Ito, J. Schlarp and G. Schitter, "System Integration and Control for 3D Scanning Laser Metrology," *IEEJ Transactions on Industrial Applications*, vol. 8, no. 2, p. 207-217, 2019. DOI: 10.1541/ieejjia.8.207